0273-2289/95/5002—0109$07.40

Simultaneous Measurement of Glucose and Glutamine in Aqueous Solutions by Near Infrared Spectroscopy

HOEIL CHUNG,[1] MARK A. ARNOLD,*[,1]
MARTIN RHIEL,[2] AND DAVID W. MURHAMMER[2]

[1]Department of Chemistry, and [2]Department of Chemical and Biochemical Engineering, The University of Iowa, Iowa City, IA 52242

Received April 26, 1994; Accepted May 25, 1994

ABSTRACT

A method is described for measuring the concentrations of both glucose and glutamine in binary mixtures from near infrared (NIR) absorption spectra. Spectra are collected over the range from 5000–4000/cm (2.0–2.5 μm) with a 1-mm optical path length. Glucose absorbance features at 4710, 4400, and 4300/cm and glutamine features at 4700, 4580, and 4390/cm provide the analytical information required for the measurement. Multivariate calibration models are generated by using partial least squares (PLS) regression alone and PLS regression combined with a preprocessing digital Fourier filtering step. The ideal number of PLS factors and spectral range are identified separately for each analyte. In addition, the optimum Fourier filter parameters are established for both compounds. The best overall analytical performance is obtained by combining Fourier filtering and PLS regression. Glucose measurements are established over the concentration range from 1.66–59.91 m*M*, with a standard error of prediction (SEP) of 0.32 m*M* and a mean percent error of 1.84%. Glutamine can be measured over the concentration range from 1.10–30.65 m*M* with a SEP of 0.75 m*M* and a mean percent error of 6.67%. These results demonstrate the analytical utility of NIR spectroscopy for monitoring glucose and glutamine levels in mammalian and insect cell cultures.

*Author to whom all correspondence and reprint requests should be addressed.

Index Entries: Glucose; glutamine; near infrared (NIR); Partial Least Squares (PLS) regression; digital Fourier filter; fed-batch bioreactor.

INTRODUCTION

A wide range of useful products are produced from microorganisms and animal cell cultures. The simplest large scale method used to produce these products is a bioreactor operating in the batch mode. Cell growth and/or product synthesis in the batch mode, however, is commonly limited by either nutrient exhaustion or inhibitory byproduct accumulation. Modified batch bioreactors, i.e., a fed-batch bioreactor, can be used to eliminate nutrient exhaustion by feeding the required nutrients at a rate equal to their consumption rate. Fed-batch bioreactors have been demonstrated to increase cell and product yields of a variety of organisms, including bacteria (*1*), yeast (*2*), insect cells (*3*), and mammalian cells (*4*). For bacteria and yeast it is usually sufficient to feed only glucose. Feeding glucose and glutamine is critical for cell growth and product production in insect (*5*) and mammalian cell cultures (*6*), in which typical glucose and glutamine concentrations are 20 and 6 m*M*, respectively. Glucose and glutamine consumption by mammalian cells, which are utilized to produce energy, is concomitant with the production of potentially inhibitory lactate and ammonium ion byproducts, respectively. Glacken et al. (*6*) demonstrated that controlled feeding of glucose and glutamine can significantly reduce lactate and ammonium ion synthesis in mammalian cell cultures. Perfusion bioreactors, with fresh medium continuously flowing through a system in which cells are retained, are alternative systems for continuously removing toxic byproducts and supplying nutrients to insect (*7*) and mammalian cell cultures (*8*). The practical application of perfusion bioreactors, however, is limited because of excessive medium consumption.

Previous use of batch, fed-batch, and perfusion systems has clearly demonstrated that a well controlled fed-batch system is the most practical for eliminating nutrient exhaustion and reducing inhibitory byproduct accumulation to increase cell product yields. Control of a fed-batch bioreactor is dependent on reliable measurements that can be used to maintain constant nutrient concentrations within the bioreactor. Enzyme-based biosensors are commonly used to quantify glutamine (*9*), glucose (*1*), and other components. Biosensors, however, suffer from limited enzyme stability and from their invasive nature, i.e., they require sample withdrawal from the bioreactor and transport to the analyzer.

An alternative method of measuring medium component concentrations is near-infrared (NIR) spectroscopy (*10*), which is noninvasive, has long term stability, and is capable of measuring many components from a single spectrum (*11,12*). Enzyme-based biosensors (*13*) have superior

detection limits compared to those of NIR spectroscopy. The detection limits of NIR spectroscopy, however, are well within the range necessary for practical applications in monitoring important components in microbial and animal cell bioreactors. NIR spectroscopy previously has been shown to be capable of accurately measuring glutamine in pure samples (*14*). In addition, binary mixtures of glucose and ammonium ion have been used to demonstrate the simultaneous measurement of these compounds with NIR spectroscopy (*14*).

In the present study the authors demonstrate the ability of NIR spectroscopy to simultaneously measure glucose and glutamine in binary mixtures composed in aqueous solutions. This is an important and necessary step toward establishing the feasibility of NIR spectroscopy in monitoring nutrients in insect and mammalian cell bioreactors. The spectra were processed by the multiple linear regression method based on the partial least squares (PLS) algorithm (*15–17*). In addition, digital Fourier filtering (*18*) was combined with PLS to improve the measurement of each component.

EXPERIMENTAL

Apparatus and Reagents

All the spectra were collected with a Nicolet 740 Fourier Transform infrared (FTIR) spectrometer (Nicolet Analytical Instruments, Madison, WI). The spectrometer was designed to operate in the NIR range by using a 250 W tungsten-halogen source, CaF_2 beam splitter and cryogenically cooled InSb detector. To isolate the spectral range 5000–4000/cm a multilayer optical interference filter (Barr Assoc., Westford, MA) was used. The temperature of the cell was controlled with a VWR 1140 refrigerated temperature bath (VWR Scientific, Chicago, IL). A 1-mm path length rectangular cell made from Infrasil quartz (Wilmad Glass Co., Buena, NJ) was used. The filled cell was positioned in a sample holder equipped with a glass-jacketed cell to control the solution temperature. The solution temperature was measured by positioning a copper-constantan thermocouple probe directly into the sample and reading the temperature from an Omega Model 670 digital meter.

All the reagents were purchased from Sigma Chemical Co. (St. Louis, MO). Buffer was prepared by dissolving 1.050 g of $NaHCO_3$ and 3.039 g of NaH_2PO_4 into 3 L of pure water obtained from a Millipore Milli-Q UF Plus water purification system and adjusting the pH to 6.35.

Procedures

Standards

Twenty-two different standard solutions of glucose ranging from 3.32–119.82 m*M* and 23 different standard solutions of glutamine ranging

from 2.20–61.30 m*M* were prepared by dissolving appropriate amounts of dried materials in buffer. Seventy different binary mixtures were randomly prepared by mixing equal volumes of glucose and glutamine standards. Therefore, the concentration of each component was half that in the original standard.

Near Infrared (NIR) Spectra

NIR spectra were obtained for each sample by placing it in the thermostatted sample holder and allowing approx 2 min for the sample to thermally equilibrate at 27°C. All single beam spectra were obtained from double-sided interferograms collected from 256 co-added scans with a spectral resolution of 1.9/cm. Single beam spectra were produced by triangularly apodized and Fourier transformed interferograms with routines provided in the Nicolet SX-FTIR Ver. 4.4 software package. In most cases, three single beam spectra were collected for each sample solution. In a few cases, only two spectra were collected. In all cases, replicate spectra were collected sequentially without removing the sample from the instrument. Background single beam spectra were collected from a plain buffer solution. Generally, a new background spectrum was collected after every fourth sample and the resulting spectrum served as the reference spectrum for subsequent sample spectra. Absorbance spectra were obtained by computing the negative logarithm of ratioed spectra. Ratioed spectra were computed by dividing each single beam sample spectrum by the appropriate single beam reference spectrum. In all, 209 absorbance spectra were obtained from the 70 unique binary mixtures of glucose and glutamine.

Spectral Processing

All the single beam spectra were subsequently transferred to an Iris Indigo computer (Silicon Graphics, Inc., Mountain View, CA) for processing. All computer software used for the spectral processing was obtained from Gary W. Small from the Center for Intelligent Chemical Instrumentation in the Department of Chemistry at Ohio University, Athens, OH. All algorithms were implemented in Fortran 77. PLS regression and Fourier filtering routines involved subroutines obtained from the IMSL software package (IMSL Inc., Houston, TX).

RESULTS AND DISCUSSION

Absorption Spectra

The spectral regions available for NIR analysis of aqueous solutions are limited by the absorption of water. Water possesses a number of strong absorption bands within the NIR region of the spectrum. One spectral window falls between the 5200 and 3800/cm absorption bands of

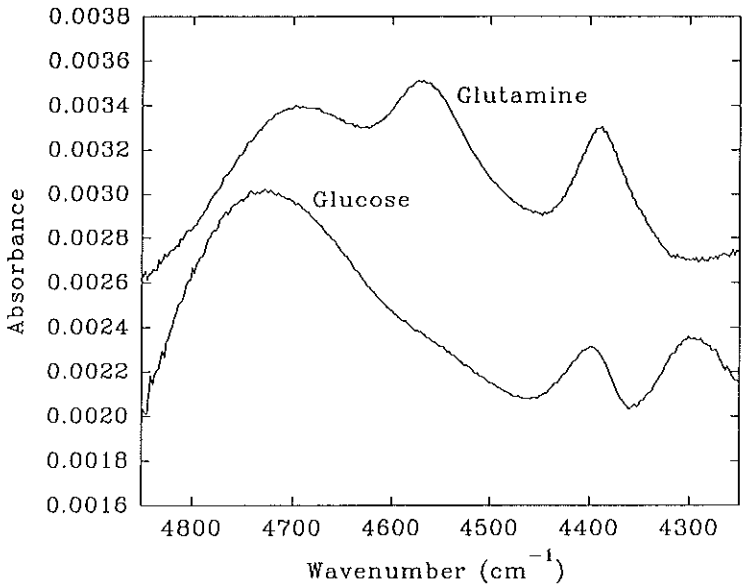

Fig. 1. NIR spectra (4850–4250/cm) of 10 m*M* glutamine and 10 m*M* glucose.

water. From a practical standpoint, this window extends from 5000–4000/cm (2.0–2.5 μm) and molecular absorptions within this window correspond to the first harmonic of combination bands associated with fundamental vibrational transitions.

Successful quantification of both glucose and glutamine from NIR absorbance spectra requires differences in the absorption properties of these molecules within the spectral window of interest. Absorption spectra for the 5000–4000/cm spectral window are presented in Fig. 1 for glucose and glutamine. Both spectra correspond to 10 m*M* solutions of the respective compound. Differences in absorption properties are most noticeable in terms of the position of the absorption bands. As pointed out before (*18,19*), glucose possesses three characteristic absorption bands centered at 4710, 4400, and 4300/cm. The spectrum for glutamine reveals three absorption bands centered at 4700, 4580, and 4390/cm. For glucose, the 4710 band has the greatest absorptivity and the 4400 and 4300 bands possess similar absorptivities. For glutamine, the 4580 and 4390 bands have similar absorptivities, which are larger than that of the 4700 band.

The spectra in Fig. 1 clearly illustrates differences in the NIR spectra of glucose and glutamine. Although the 4400 band of glucose overlaps with the 4390 band of glutamine and the 4710 band of glucose is close to the 4700 band of glutamine, the 4300 and 4580 bands differ considerably and these differences should provide the information required to quantify both species in solution. Nevertheless, the overlapping nature of these spectra motivates the use of multivariate regression procedures to

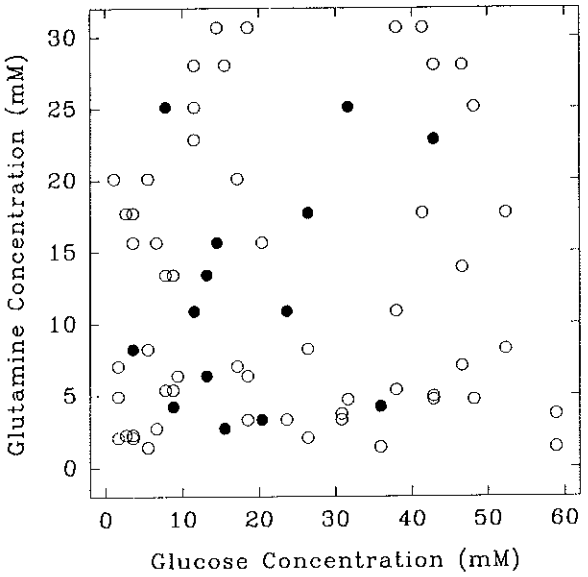

Fig. 2. Correlation plot for glucose and glutamine concentrations in standard solutions for calibration (open circles) and prediction (solid circles).

separate the two components. PLS regression has been used to generate calibration models for both analytes. In addition, the utility of a Fourier filtering preprocessing step has been evaluated as a means for improving the quality of the calibration model by removing noise and baseline variations from the raw spectra.

PLS Calibration Models

PLS is a powerful method for extracting concentration information from minute spectral variations (*15–17*). In fact, the PLS algorithm is designed to correlate spectral variations with concentration variations. When developing a calibration model based on a set of binary mixtures, it is critical that the concentration distribution is random within the set of calibration standards to the extent that there is no correlation between the concentrations of the two analytes. If such a correlation exists, then the PLS algorithm will incorporate this codependency within the calibration model, which will result in systematic errors for subsequent samples that do not possess this interrelationship.

The combinations of glucose and glutamine concentrations in the set of standards used in this study were obtained by mixing solutions randomly. The resulting glucose concentrations ranged from 1.66–59.91 m*M* and the glutamine concentrations ranged from 1.10–30.65 m*M*. Colinearity between the glucose and glutamine concentrations was evaluated by analyzing a correlation plot produced by plotting the concentration of glutamine versus that for glucose in each standard solution. Figure 2 shows the correlation plot for the data set used in this study. Inspection reveals no correla-

tion between the two concentrations. A linear regression analysis of these data results in an R-square value of only 0.00167. The same type of plot was prepared with subsets of these data to show the relationship between concentrations in solutions used for calibration and prediction. Again, no correlation is indicated by inspection and the respective R-square values are 0.00018 and 0.08850.

PLS calibration models were generated by analyzing a fraction of the whole data set, which was composed of 209 spectra from 70 binary mixtures. The calibration data set was composed of 168 spectra from 56 of the mixtures. The remaining 41 spectra, corresponding to the remaining 14 mixtures, were used to test the validity of the resulting calibration model by serving as a prediction data set.

The number of PLS factors and the spectral range represent the two critical parameters that must be established for the PLS algorithm. The optimum number of factors can be identified as the number of factors that gives a minimum standard error of prediction (SEP). The SEP directly indicates the ability of the calibration model to predict concentrations accurately from spectra in the prediction data set (*19*).

In addition, the spectral range can dramatically affect the quality of a calibration model (*19*). Previous work to measure glucose in biological fluids by NIR spectroscopy indicates that the best spectral ranges to investigate correspond to those that contain absorption bands for the compound of interest. In this work, five and six different spectral ranges were tested for glutamine and glucose, respectively. The widest spectral range used for glucose and glutamine ranged from 4850–4250/cm and 4800–4250/cm, respectively. In both cases, no absorption bands are located outside this range (i.e., from 5000 to 4850 and from 4250–4000/cm). In addition, the light intensity is very low outside this range which results in large noise levels. Previous work illustrates that removing this noise by cutting out noisy spectral regions improves the quality of the calibration model (*19*). For glutamine, the following additional spectral regions were tested: 4700–4320, 4650–4320, 4700–4450, and 4450–4320/cm. The first two correspond to ranges wide enough to incorporate information from both the 4580 and 4390 absorption bands, but slightly smaller than the widest range tested. The third and fourth ranges correspond to the 4580 and 4390/cm absorption band, respectively. For glucose, the following additional ranges were tested: 4850–4350, 4470–4250, 4850–4470, 4470–4350, and 4350–4250/cm. The first two of these regions isolate two of the three absorption bands. The first isolates the 4710 and 4400 bands and the second isolates the 4400 and 4300 bands. The last three regions focus on single bands (4710, 4400, and 4300, respectively).

The optimum number of PLS factors was identified for each spectral range and each analyte. The results of this experiment are summarized in Table 1 and a typical result is illustrated in Fig. 3. In this figure, the standard errors of calibration (SEC) and prediction (SEP) are plotted as functions of the number of PLS factors used for the determination of glucose

Table 1
Results from Calibration Models for Glucose and Glutamine Based on PLS Regression

Spectral range/cm	Number of factors	SEC, mM	SEP, mM
Glucose			
4850–4250	7	0.67	0.42
4470–4250	6	0.64	0.41
4850–4350	7	0.73	0.48
4470–4350	9	0.68	0.64
4350–4250	5	0.91	0.55
4850–4470	6	0.85	0.48
Glutamine			
4700–4320	8	0.67	0.80
4700–4450	6	0.78	1.01
4450–4320	7	0.74	1.06
4650–4320	8	0.61	0.96
4800–4250	8	0.70	0.86

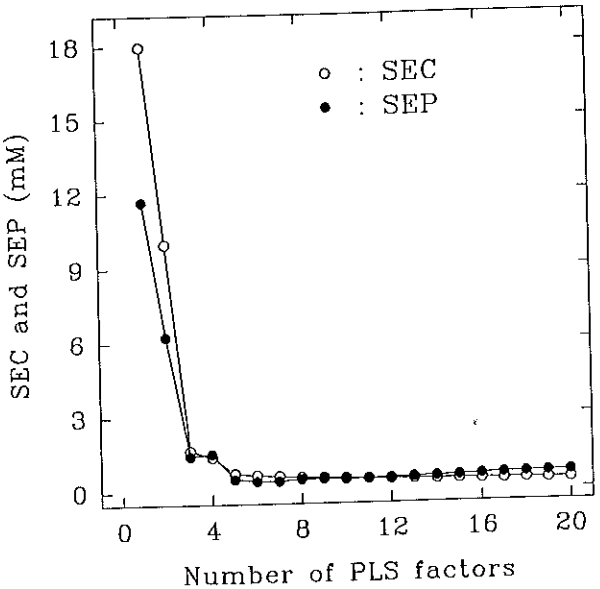

Fig. 3. The effect of number of PLS factors on SEC and SEP for glucose measurement in the spectral range 4470–4250/cm.

with the 4470–4250/cm spectral range. As expected, both the SEC and SEP decrease sharply at the beginning as more of the analyte-dependent spectral variation is incorporated into the calibration model. After the first six factors, or so, there is little improvement in either the SEC or SEP. As the number of factors is increased further, the SEC continues to decrease,

albeit only slightly; where as, the SEP actually begins to increase slightly. The point were the SEP begins to increase indicates that the data have been overmodeled by incorporating spectral variation into the calibration model that is not present in the prediction data and, therefore, does not correspond to the analyte of interest.

The values in Table 1 indicate that the best calibration models for glucose are obtained with spectral ranges of 4850–4250 and 4470–4250/cm. This first range incorporates all three glucose absorption bands, whereas the second range includes only the 4400 and 4300 bands. In each case, models generated from only one absorption band performed significantly worse compared to models built with multiple absorption bands. The highest SEP is associated with the model constructed with only the 4400 band. This band was identified as the best feature for the NIR quantification of glucose in biological fluids such as plasma (*20*) and protein containing solutions (*19*). In this present study, however, the 4400 band does not provide sufficient information because of the overlapping 4390 band associated with glutamine.

The best combination of lowest SEP and fewest number of PLS factors is obtained with the 4470–4250/cm spectral range, which corresponds to a combination of the 4400 and 4300 glucose absorption bands. A concentration correlation plot is presented in Fig. 4 for this calibration model. In this figure, the glucose concentration obtained from the calibration model is plotted versus the known glucose concentration of the standard solution. Two plots are provided which correspond to the calibration and prediction data sets. The ideal response is indicated by the unity line. These data fall very close to the ideal line. A linear regression analysis of these data reveals slopes of 0.999 ± 0.003 and 1.005 ± 0.004 and y-intercepts of 0.03 ± 0.62 and -0.13 ± 0.33 m*M* for the calibration and prediction data, respectively. Glucose concentrations in the prediction data set were accurately predicted with a 0.41 m*M* SEP and a 2.21% mean percent error.

The best calibration model for glutamine is also obtained with a wide spectral range. The lowest SEP corresponds to a combination of eight PLS factors and the 4700–4320/cm spectral range. The resulting concentration correlation plots are provided in Fig. 5. Again, the data fall close to the ideal line. Regression analysis indicates slopes of 0.995 ± 0.005 and 0.994 ± 0.016 as well as y-intercepts of 0.06 ± 0.65 and 0.21 ± 0.30 m*M* for the calibration and prediction data, respectively. The SEP and mean percent error are 0.80 m*M* and 8.17% for this best model. As with the glucose analysis, the smaller spectral regions corresponding to individual absorption bands result in inferior models.

The prediction ability of the glucose models is better than those for glutamine. Glucose can be predicted with superior accuracy and fewer numbers of PLS factors. Nevertheless, both glucose and glutamine can be measured with sufficient accuracy for bioreactor monitoring.

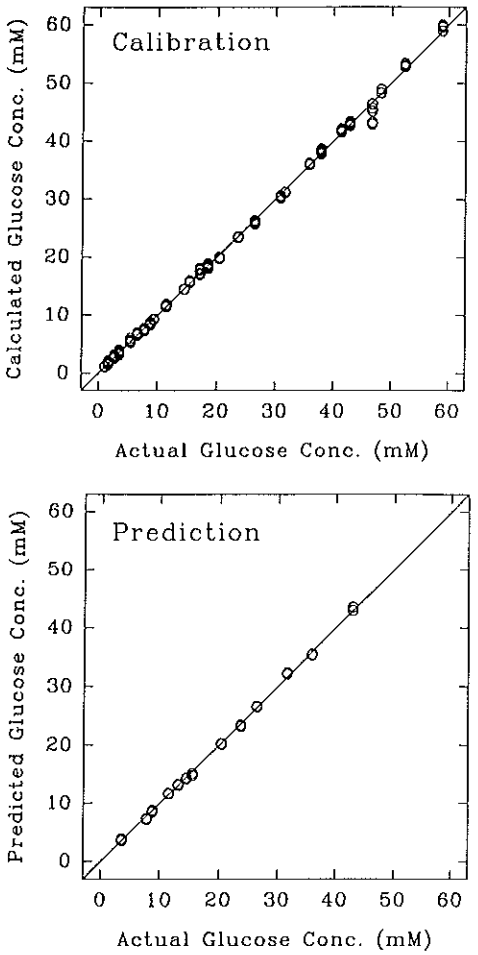

Fig. 4. Glucose concentration correlation plots for calibration (top) and prediction (bottom) using a spectral range 4470–4250/cm and six PLS factors.

PLS Combined with Digital Filtering

Our previous work with clinical glucose measurements (*18–20*) indicates that digital filtering before PLS regression can significantly improve the prediction accuracy by selectively eliminating spectral noise and baseline variations. This previous success motivated us to explore the utility of digitally filtering the spectra before the PLS regression.

The digital filter used in this work is a Fourier filter that selectively passes spectral features according to the spectral band shapes. Briefly, the Fourier filtering process involves performing a Fourier transform of the raw absorbance spectrum. This Fourier transformation step treats the absorbance spectrum as a signal vs time plot. The original raw spectrum can be thought of as the superposition of a series of sine waves. Noise

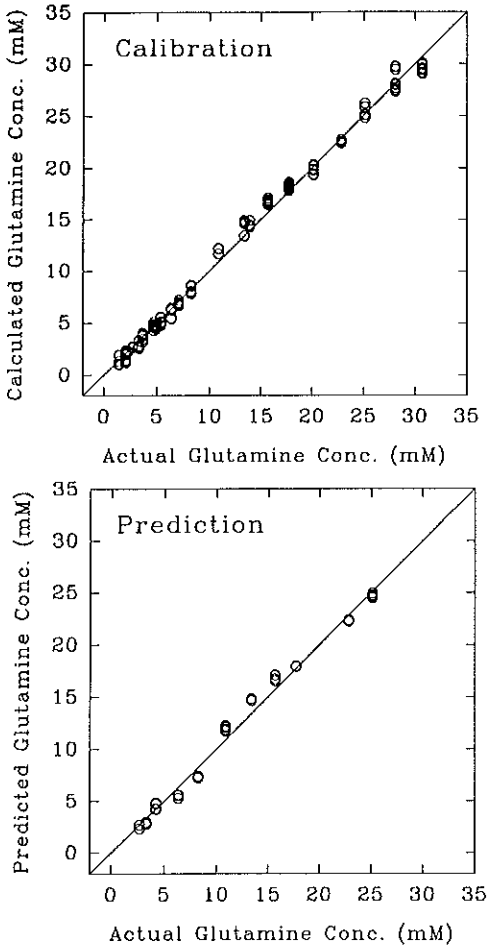

Fig. 5. Glutamine concentration correlation plots for calibration (top) and prediction (bottom) using a spectral range 4700–4320/cm and eight PLS factors.

corresponds to high frequency sine waves, baseline variations correspond to low frequency sine waves, and the molecular absorption bands correspond to sine waves with intermediate frequencies. The Fourier transformation process separates the combination of sine waves according to their frequencies (termed digital frequencies). The filtering process involves multiplying the transformed spectrum by a Gaussian function, thereby weighting the information under the Gaussian. The Gaussian response function is defined by the mean position of the Gaussian along the digital frequency axis and the standard deviation of the Gaussian that defines the width of the filter. The mean position must be set so the filter weights the molecular absorption features within the spectrum. The standard deviation width must be set to maximize the analyte-dependent information that passes through the filter. If the Gaussian function is too

wide, noise will pass through the filter but if it is too narrow, analyte-dependent information will be lost. After the multiplication step, the altered spectrum is subjected to an inverse transformation to return the data to the original data domain of an absorbance spectrum.

The key to successful digital filtering is identifying the ideal mean position and standard deviation width for the Gaussian response function. A method described before has been used in this work (*19,20*). Basically, this method involves constructing and testing PLS regression models for all combinations of mean positions and standard deviation widths for the Gaussian response function. The spectra are filtered and the resulting altered spectra are used to generate a PLS calibration model with a given number of factors and spectral range. An independent data set of spectra is used to evaluate the prediction ability of the resulting model. A response function is computed as the reciprocal of the sum of the mean square calibration error and the mean square prediction error (1/[MSE + MSPE]). A response surface is then generated by plotting the mesh corresponding to the response function vs the mean position and standard deviation widths of the Gaussian shaped filter. The morphology of the surface is examined and the optimum Gaussian function parameters are identified as the maximum feature on the surface. This maximum position corresponds to the lowest sum of mean square errors of calibration and prediction.

Sample response surfaces for glucose and glutamine are presented in Fig. 6. These surfaces were generated by using 4 PLS factors with the spectral range from 4850–4250/cm for glucose and 5 PLS factors with the spectral range from 4700–4320/cm for glutamine. Response functions were computed for all combinations of means ranging from 0–0.1 (0.001 step size) and standard deviations ranging from 0–0.02 (0.001 step), which corresponds to the construction and evaluation of 2000 individual calibration models. Both surfaces show an optimal location (peak) along a ridge of high values. The optimum mean-standard deviation pairs are 0.030–0.005 f for glucose and 0.018–0.004 f for glutamine. Similar surfaces were obtained for the other spectral ranges. Optimal filter parameters found for glucose and glutamine are summarized in Table 2 for different spectral ranges.

The optimum filters for glucose and glutamine are quite similar which indicates that these filters are not able to discriminate between these two compounds based on differences in their absorption spectra. In fact, each filter passes a significant amount of information related to the other compound. Fig. 7 illustrates results obtained after passing raw spectra through filters optimized for glucose (Fig. 7A) and glutamine (Fig. 7B) when the "principal" analyte concentration is held constant while the "interfering" analyte concentration changes. The spectra in Fig. 7A correspond to filtered spectra after passing through the optimal Fourier filter for glucose when the glucose level is maintained at 3.55 mM and the glutamine concentrations are 8.22, 15.65, and 17.71 mM. Variations in

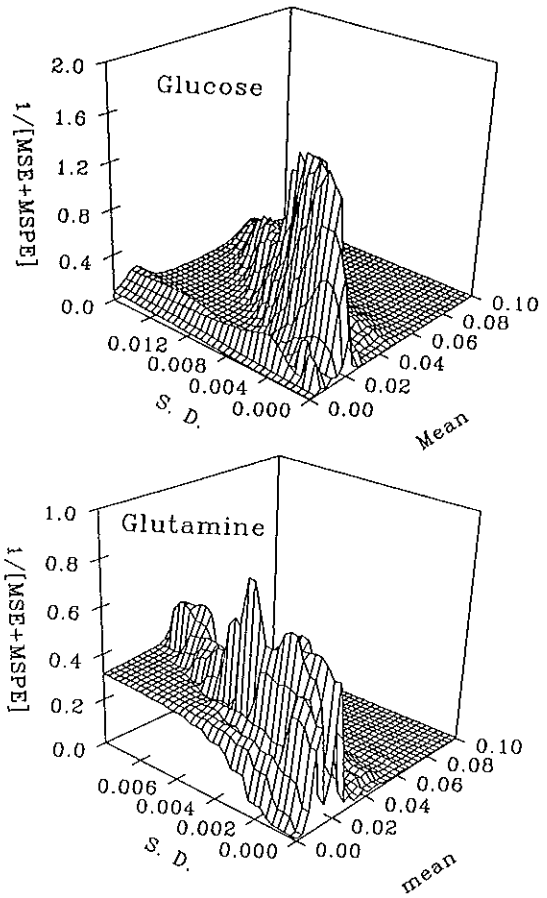

Fig. 6. Response surface maps for the optimization of Fourier filter parameters for glucose and glutamine.

Table 2
Calibration Models for Glucose and Glutamine Based on Fourier Filtering Combined with PLS Regression

Spectral range/cm	Mean	Standard deviation	Number of factors	SEC, m*M*	SEP, m*M*
Glucose					
4850–4250	0.030	0.005	6	0.63	0.32
4470–4250	0.023	0.003	6	0.65	0.38
4850–4350	0.026	0.004	6	0.63	0.33
4700–4250	0.022	0.003	6	0.70	0.35
Glutamine					
4700–4320	0.018	0.004	7	0.77	0.75
4700–4450	0.018	0.004	9	0.80	0.84
4450–4320	0.019	0.002	8	0.87	0.90
4650–4320	0.019	0.004	5	0.87	0.86
4800–4250	0.024	0.005	7	0.87	0.88

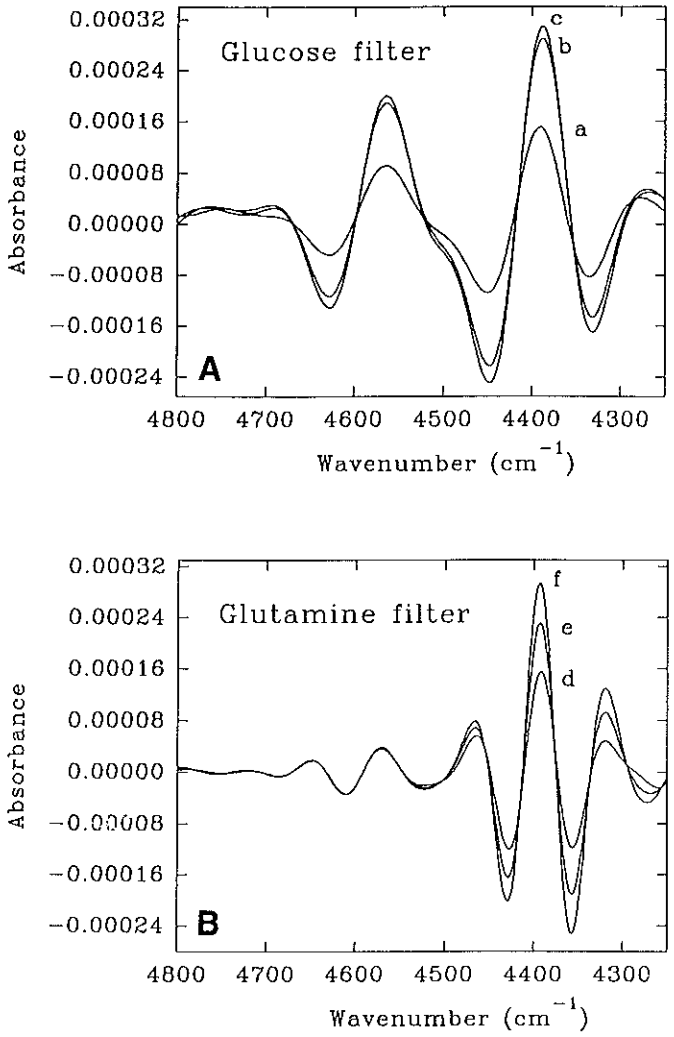

Fig. 7. Spectra after Fourier filtering using the optimum filter for glucose (**A**) and optimum filter for glutamine (**B**). Spectra a, b, and c correspond to a glucose concentration of 3.55 m*M* and glutamine concentrations of 8.22, 15.65, 17.71 m*M*, respectively. Spectra d, e, and f correspond to a glutamine concentration of 25.11 m*M* and glucose concentrations of 11.52, 31.61, 48.15 m*M*, respectively.

signals at 4390 and 4580/cm correspond to glutamine concentration variations. Glucose information is likewise passed through the glutamine filter. Fig. 7B presents spectra after filtering with the glutamine optimized Fourier filter for solutions with a constant glutamine level (25.11 m*M*) and varying glucose concentrations (11.52, 31.61, and 48.15 m*M*). The varia-

tion in peak height at 4400 and 4300/cm correspond to the changes in glucose concentration. Clearly, glucose information passes through the glutamine filter and glutamine information passes through the glucose filter. Consequently, multivariate analysis is needed to quantify both compounds even after Fourier filtering.

Calibration models based on the combination of Fourier filtering and PLS regression are slightly better for both glucose and glutamine compared to models based solely on PLS alone. Results from Fourier filter/PLS calibration models are summarized in Table 2 for glucose and glutamine. The performance of the model is relatively insensitive to spectral range. SEP values are generally smaller and fewer number of PLS factors are required compared to models based on PLS alone.

Calibration Models for Glucose and Glutamine

The best performance for glucose was obtained with the 4850–4250/cm spectral range, six PLS factors, and a Fourier filter defined by a mean of 0.030 *f* and a standard deviation of 0.005 *f*. The corresponding SEC, SEP and mean percent error are 0.63 m*M*, 0.32 m*M*, and 1.84%, respectively. For glutamine, the best performance used the spectral range from 4700–4320/cm, 7 PLS factors, and Fourier filter parameters of 0.018 and 0.004 *f*. The corresponding SEC, SEP, and mean percent error are 0.77 m*M*, 0.75 m*M*, and 6.67%, respectively. Fig. 8 presents concentration correlation plots for these two best calibration models. In both cases, the calibration and prediction data sets fall close to the ideal line with no indication of deviation. Regression analysis of the glucose correlation plot indicates slopes of 0.999 ± 0.003 and 1.005 ± 0.005 as well as *y*-intercepts of 0.03 ± 0.62 and −0.13 ± 0.33 m*M* for the calibration and prediction data, respectively. For glutamine, regression analysis indicates slopes of 0.994 ± 0.006 and 1.000 ± 0.015 as well as *y*-intercepts of 0.07 ± 0.75 and 0.25 ± 0.73 m*M* for the calibration and prediction data, respectively.

The presence of glucose had no apparent adverse effect on our ability to measure glutamine concentrations. A three-dimensional scatter plot was prepared by plotting the measured percent error of prediction for glucose as a function of glucose concentration and as a function of glutamine concentration (plot not shown). Although there was an increase in the percent error at lower concentrations of glucose, the percent error was not influenced by the concentration of glutamine. We had suspected that larger percent errors would be observed for low levels of glucose in the presence of high concentrations of glutamine. Inspection of the data, however, indicates no bias of this fashion.

Likewise, there does not seem to be an adverse effect by glucose on our ability to measure glutamine. Percent errors at low glutamine concentrations are essentially the same regardless of the glucose concentration.

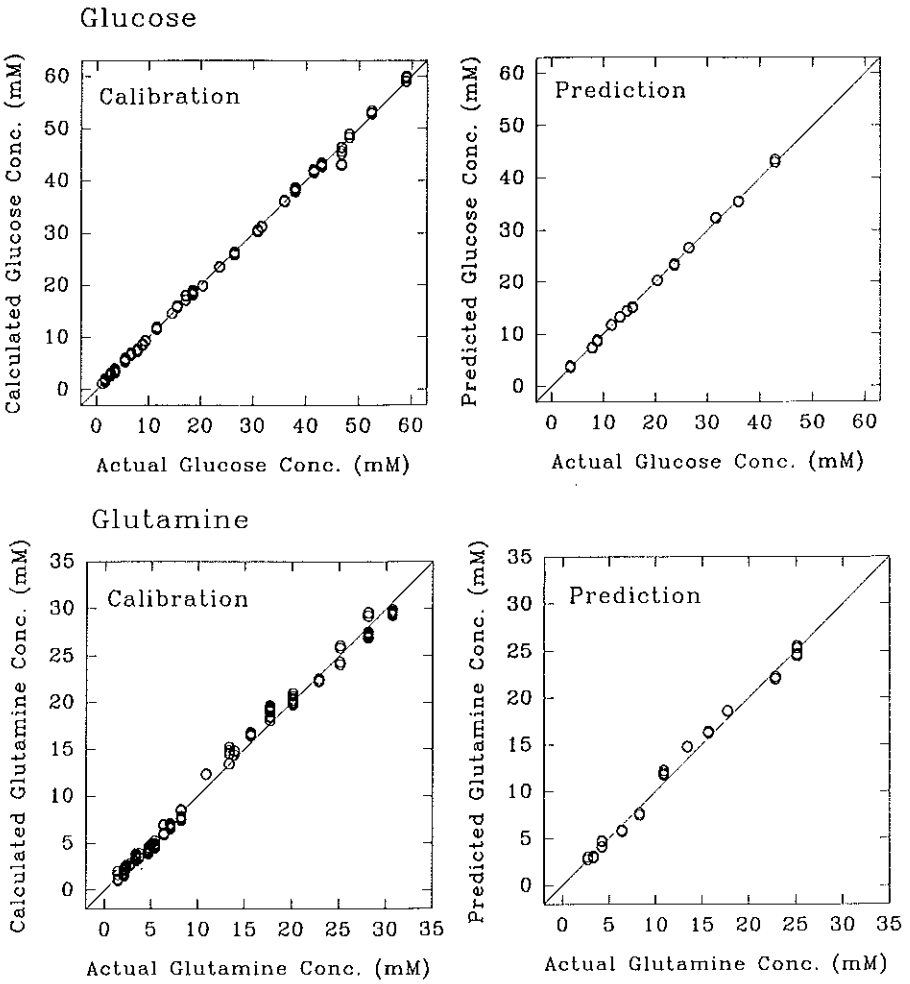

Fig. 8. Concentration correlation plots for glucose (top) and for glutamine (bottom) by coupling Fourier filtering with PLS regression.

CONCLUSION

The simultaneous measurement of glucose and glutamine concentrations with near infrared (NIR) spectroscopy was demonstrated. Research currently being conducted in our laboratories is utilizing NIR spectroscopy to analyze mixtures of increasing complexity with the ultimate goal of simultaneously measuring glucose, glutamine, and other components in actual mammalian and insect cell culture media. The standard error of prediction found in the present research of 0.32 and 0.75 m*M* for glucose and glutamine, respectively, are well within the precision levels necessary for the practical monitoring of these components in mammalian and insect cell cultures. The use of NIR spectroscopy to monitor these cell cultures will provide many advantages over the use of biosensors because

NIR spectroscopy is noninvasive, nondestructive, and can simultaneously determine the concentration of many components. Such a monitoring system will greatly benefit efforts to improve cell culture productivity by using fed-batch cultures in which nutrient deprivation and toxic by-product accumulation can be minimized.

ACKNOWLEDGMENT

The authors thank Gary W. Small in the Center for Intelligent Chemical Instrumentation at Ohio University for providing the software for the spectral analysis and Geng Lu for his assistance in collecting some spectra. Portions of this work were supported from a grant by NIH (DK-45126).

REFERENCES

1. Kleman, G. L., Chalmers, J. J., Luli, G. W., and Strohl, W. R. (1991), *Appl. Environ. Microbiol.* **57**, 910–917.
2. Dairaku, K., Yamasaki, Y., Kuri, K., Shioya, S., and Takamatsu, T. (1981), *Biotechnol. Bioeng.* **23**, 2069–2081.
3. Reuveny, S., Kim, Y. J., Kemp, C. W., and Shiloach, J. (1993), *Biotechnol. Bioeng.* **42**, 235–239.
4. Fike, R., Kubiak, J., Price, P., and Jayme, D. (1993), *BioPharm* **6(8)**, 49–54.
5. Reuveny, S., Kemp, C. W., Eppstein, L., and Shiloach, J. (1992), *Ann. NY Acad. Sci.* **665**, 230–237.
6. Glacken, M. W., Fleischaker, R. J., and Sinskey, A. J. (1986), *Biotechnol. Bioeng.* **28**, 1376–1389.
7. Fertig, G., Rahn, H. P., Angermann, A., Kloppinger, M., and Miltenburger, H. G. (1993), *Cytotechnology* **11**, 67–75.
8. Takazawa, Y. and Tokashiri, M. (1989), *Appl. Microbiol. Biotechnol.* **32**, 280–284.
9. Cattaneo, M. V. and Luong, J. H. T. (1993), *Biotechnol. Bioeng.* **41**, 659–665.
10. Burns, D. A. and Ciurczak, E. W. (1990), *Handbook of Near-Infrared Analysis*, Marcel Dekker, New York.
11. Wetzel, D. L. (1983), *Anal. Chem.* **55**, 1165A–1176A.
12. Dotzlaw, G. and Weiss, M. D. (1993), *Chem. Eng. Prog.* **89(9)**, 42–45.
13. Reach, G. and Wilson, G. S. (1992), *Anal. Chem.* **64**, 381A–386A.
14. He, M., Lorr, D., and Wang, N. S. (1993), *Near-infrared spectroscopy for on-line bioreactor monitoring*, presented at the 1993 AIChE National Meeting, St. Louis, MO.
15. Geladi, P. and Kowalski, B. (1986), *Anal. Chim. Acta.* **185**, 1–17.
16. Beebe, K. R. and Kowalski, B. (1987), *Anal. Chem.* **59**, 1007A–1018A.
17. Haaland, D. M. and Thomas, E. V. (1988), *Anal. Chem.* **60**, 1193–1202.
18. Arnold, M. A. and Small, G. W. (1990), *Anal. Chem.* **62**, 1457–1464.
19. Small, G. W., Marquardt, L. A., and Arnold, M. A. (1993), *Anal. Chem.* **65**, 3271–3278.
20. Arnold, M. A., Marquardt, L. A., and Small G. W. (1993), *Anal. Chem.* **65**, 3279–3289.